Proposal to PAC-21 Hall A, Jefferson Lab

Investigation of Short-Range Correlations in the ^{3}He(e, e′pp)n_{sp} Reaction at x>1 (An Update to E99-102 and LOI-01-103)

E.J. Brash, S. Dumalski, G.M. Huber, N. Knecht, V. Kovaltchouk, A. Kozlov, Sh. Li, G.J. Lolos, Z. Papandreou, A. Shinozaki
University of Regina

J.R.M. Annand, D. Hamilton, D. Ireland, G. Rosner
University of Glasgow

W. Bertozzi, S. Gilad, S. Sirca, Z. Zhou
Massachusetts Institute of Technology.

E. Piasetzky
Tel Aviv University

M. Epstein, D. Margaziotis
California State University, Los Angeles

M.K. Jones, D.W. Higinbotham, S.A. Wood
Jefferson Laboratory

B. Anderson, J. Watson, W-M. Zhang
Kent State University

R. Gilman, C. Glasshauser, G. Kumbartzki, R. Ransome, X. Xiang
Rutgers University

A.J. Sarty
St. Mary's University

V.Nelyubin
University of Virginia & St.Petersburg Nuclear Physics Institute

December 3, 2001

Abstract

We propose to investigate short-range correlations (SRC) in inelastic electron scattering via the two proton knockout reaction $^3\mathrm{He(e,e'pp)n_{sp}}$. Such correlations have a specific dynamical signature in the ground state wavefunction of the target nucleus which bridges the gap between nucleonic and quark degrees of freedom. As such, these measurements will provide severe constraints on existing theoretical models which employ realistic NN potentials, while, at the same time providing the impetus for new calculations.

Our objectives will be accomplished by measuring the cross section for this reaction on the low ω side of the quasi-elastic peak, i.e. at x>1, as a function of the internal momenta of the target nucleus. It is generally acknowledged that the $(e, e'pp)$ channel is an excellent candidate for probing SRC, however, any experiment which aims to address this physics must be designed carefully in order to minimize competing processes. The key in our approach is to choose a kinematic region where meson exchange currents and isobar currents are expected to be minimal, and where the SRC signature is the cleanest and strongest. The optimal kinematical setting for such a measurement is that in which the two ejected protons egress nearly parallel and antiparallel, respectively, to the momentum transfer vector prior to absorption, and the energy transfer region lies on the lower side of the quasi-elastic peak, with the **missing momentum of the neutron confined to spectator values.** Thus, specifically, we are looking for an enhancement in the $^3\mathrm{He(e,e'pp)n_{sp}}$ cross-section in these kinematics compared to what one might expect by combining $^3He(e, e'p)$ cross-sections with phase-space calculations of the pn recoil system. Such an enhancement is indicative of the presence of strongly correlated pp pairs in the initial ground state wavefunction.

The ^{3}He nucleus has been selected because it is the lightest nuclear system for which the reaction can proceed, realistic wavefunctions are available, and a triple coincidence renders the experiment kinematically complete.

We propose to carry out these measurements using the two high resolution spectrometers in Hall A for detecting the scattered electron and the forward proton. The second proton will be detected using the soon-to-be-commissioned BigBite spectrometer. We request 240 hours of beamtime at a beam current of 100 μA.

1 Introduction

Electromagnetic probes are ideal for the study of the hadronic structure of nuclei and elementary particles. Indeed, electro- and photo-nuclear experiments have provided us with a wealth of information and have helped deepen our understanding of subnuclear degrees of freedom.

With the advent of high-energy, high-intensity electron accelerators operating with a continuous wave (CW) beam (nearly 100% d.f.), we are well poised to carry out many important and very interesting experiments in this field, especially in the transition region between intermediate energy and particle physics. Short-range correlations is one such topic which has recently generated much interest in the electromagnetic scientific community [1, 2].

It is important to define the term SRC here, in the context of this proposal. The particular correlations to which we refer correspond to configurations in the target ground-state wavefunction where two nucleons are in very close spatial proximity to one another. In a more fundamental picture, this corresponds to an overlap of the quark bags of the individual nucleons at extremely small internucleon distances (ca. 0.2-0.3 fm). This part of the target wavefunction cannot be described by traditional meson exchange, as evidenced by the difficulties that traditional boson exchange models have in describing the short-range character of the NN interaction. As such, SRC bridge the gap between nucleonic and quark degrees of freedom.

In this proposal, we are not seeking to investigate traditional two-body correlations (2BC), such as meson exchange currents (MEC) or isobar currents (IC). These 2BC are relatively well understood, thanks to the wealth of data from pion and real-photon absorption, as well as the recent measurements NIKHEF, MAINZ, and elsewhere with virtual photons, and are the subject of other experimental efforts at Jefferson Lab. Although the 2BC measurements themselves provide valuable cross-checks for the few-body calculations that may assist in the interpretation of the results of this experiment, here, **we have chosen kinematics so as to suppress 2BC and all other mechanisms competing with SRC.**

There are a number of approved experiments at Jefferson Lab with similar goals to ours. In particular, our proposal is closely related to E01-015, which was approved to measure NN correlations in the $^{12}C(e, e'pN)$ reaction. The salient features of these experiments, and their comparison and complementarity to ours, will presented later in this proposal.

2 Correlations in Nuclei

2.1 Contributing Mechanisms

The successes of electro-nuclear scattering experiments, in terms of the resultant physics which has been extracted, are manifested in the simplicity and exactness of the electron-nucleon coupling mechanism. The *e-nucleon* and *e-nucleus* interactions

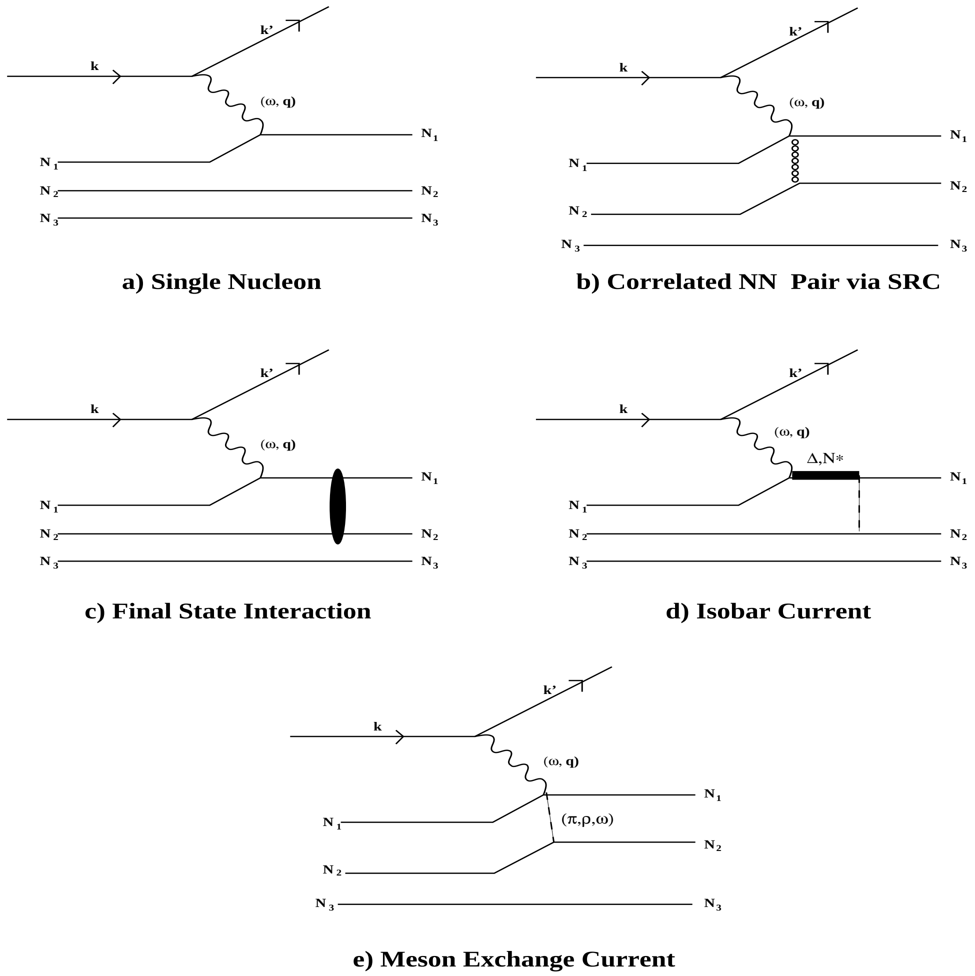

Figure 1: Diagrams contributing to the $^3\mathrm{He(e,e'pp)n}$ channel.

are largely based on diagrams such as the one shown in Figure 1a, in which the energy and momentum of the exchanged virtual photon is transfered to a single nucleon, with the remaining (A-1) nucleons behaving as spectators. This mechanism is perturbative and allows the separation of effects due to the reaction mechanism from those due to nuclear structure, in the plane wave impulse approximation (PWIA) framework.

Even in deuterium, however, the need for other diagrams arose in order to account for the experimental data [3], such as IC like the Δ or N^* resonances (Figure 1d) as well as non-resonant MEC (Figure 1e). Additionally, final state interactions (FSI) may become involved (Figure 1c). These FSI modify the four-momentum of the struck nucleon, thus altering the flux in any particular kinematical region, and complicate the interpretation of the results. The PWIA picture breaks down if FSI are large.

The existence of traditional 2BC (Figures 1d and 1e) has been firmly established in pion absorption measurements, spanning the last three decades. Recent real photon absorption results confirm this [4, 5]. It should be noted that pion- and real photo-absorption, at energies of $\geq$ 100 MeV, probe primarily NN and NNN correlations, due to the large momentum mismatch in these reactions. In addition, evidence for correlations has also been found via the $(e, e'p)$ reaction [6], in which the incoming virtual photon was interpreted to interact with a correlated nucleon pair. The characteristics of pions and real and virtual photons establish them as complimentary tools in the investigation of two-nucleon interactions. For a more detailed comparison of these probes, the reader is directed to reference [7].

However, none of these approaches distinguishes or is able to separate SRC from 2BC (Figure 1b from Figures 1d, e). Theoretically, a re-examination of $(e, e'p)$ and other data from Bates by Schiavilla [8], based on Coulomb sum rules and proton-proton correlations, has thus presented only *indirect* evidence for SRC, because of this inability to separate the different contributions.

2.2 Theoretical Issues

The information obtained so far on correlations from $(e, e'p)$ and most recently from $(e, e'pp)$ reactions has been instructive in many ways. In particular, it has been put forth by a number of theoretical groups that much can be learned from studying the $^3\mathrm{He}(\mathrm{e}, \mathrm{e}'\mathrm{pp})\mathrm{n}$ channel, which is the best candidate for two-proton ejection investigations, provided that the two detected protons are those which were initially correlated in the ground state of the nucleus [9]-[13].

In particular, on the low ω side of the quasielastic peak, where MEC and IC are expected to have negligible contribution to the cross section, Glöckle and collaborators [12] have shown that it is possible to make full final state interaction calculations, and that any excess strength in the $^3\mathrm{He}(\mathrm{e}, \mathrm{e}'\mathrm{pp})\mathrm{n}$ cross-section should be entirely due to SRC processes. This kinematic region has also been suggested by Frankfurt *et al.* [10].

As mentioned above, at the quark level, SRC manifest themselves as overlap of the quark-filled bags. Theoretical calculations, based on nucleonic degrees of freedom, do not look at things in this way. The Bochum group, who calculate the $(e, e'pp)$ cross-sections within a nucleonic framework, assemble a number of ideas. The interaction with the virtual photon is well-understood, and more importantly FSI are treated completely, by solving the scattering theory problem exactly. However, while the target spectral function is calculated in an exact manner, at the heart of it is an NN potential that is phenomenological and based on meson exchange. As such, the short-range character of the interaction is implicitly built into the NN potential and cannot be decoupled. As anillustration of this point, we point to a comparison of theoretical models based on realistic NN potentials to $^4\mathrm{He}(\mathrm{e}, \mathrm{e}'\mathrm{p})^3\mathrm{H}$ data [14]. In this paper, the authors show that at high missing recoil momentum, NN potentials, which are known to describe short-range behavior well, fare better in the description of the data.

This sensitivity is also shown in Fig. 2, where we show calculations of the *pp*

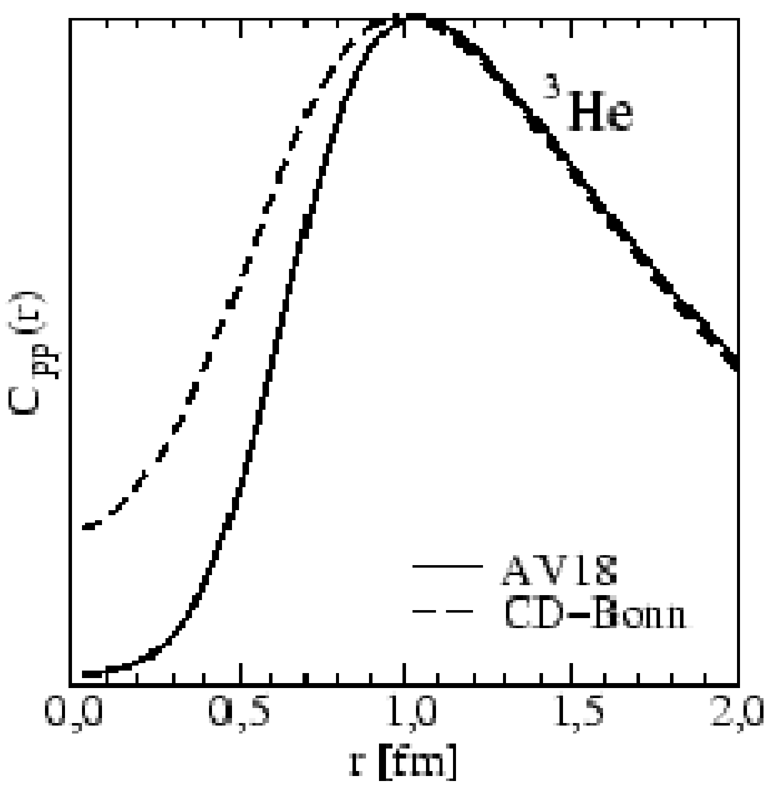

Figure 2: The pp correlation function for ^{3}He from Ref. [12]

correlation function for ^3He. We note the sensitivity at small r to the particular NN potential which is used. In this case, the two potentials handle the short-range repulsive core in different ways. As mentioned above, in this experiment we probe momenta which correspond to separation distances in the 0.2-0.3 fm range.

Of course, interpretation of our results will be more involved. As Glöckle points out in Ref. [12], the above correlation function is not an observable, however, it does enter directly into observable response functions. Also, he notes the importance of including FSI effects in such calculations. He states:

> "Precise experimental data on two-nucleon emissions induced by real and virtual photons on ^{3}He will be a very important test ground to probe nuclear forces, correlated wave functions and currents. At present the 3N system is the only case where FSI is fully under control (below the pion threshold) and appears therefore especially promising to probe our present day understanding of nuclear dynamics."

Another issue which must be addressed is the range of appicability of fully non-relativistic calculations such as those of the Bochum group. Admittedly, no framework exists to solve exactly this scattering problem in a Lorentz-covariant manner. However, certain parts of the calculation - especially the kinematics and calculation

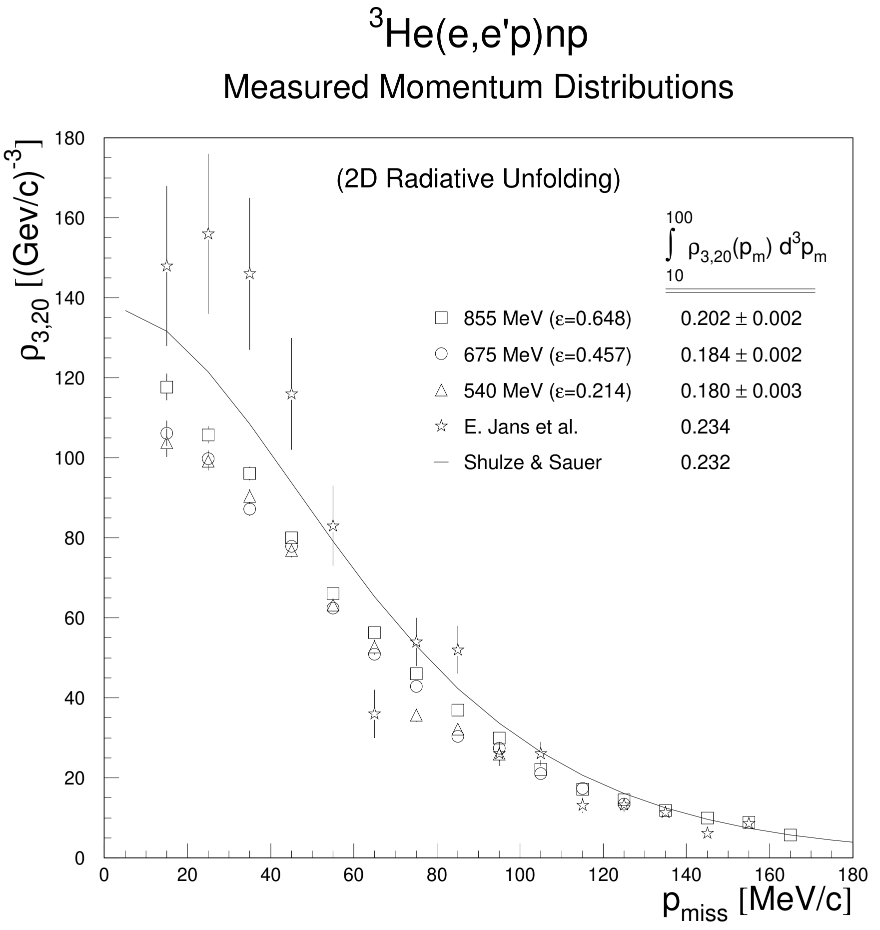

Figure 3: Momentum distribution for the $^3He(e,e'p)pn$ continuum from [15]

of the phase-space factor - can be performed with relativistic kinematics. Currently, Glöckle and collaborators are pursuing a more advanced dynamical picture which would include relativity in the instant form of a Hamiltonian formalism. We hope that results from this experiment will encourage the theory community to extend current models to include such effects.

2.3 Suppression of MEC and IC

It has been shown in measurements at Mainz (see Fig. 3) that the longitudinal and transverse nature of the $^3He(e,e'p)pn$ cross section is well described by the elementary $e-p$ cross section at the top of the quasi-elastic peak. No surplus transverse strength, as evidenced by the consistency of the cross section data over a wide range of ϵ values, which one would expect in the the presence of 2BC, was observed. In this experiment, we will make measurements on the lower ω side of the

QE peak, and thus 2BC are expected to be even less important.

The choice of the $^3\mathrm{He}(\mathrm{e},\mathrm{e}'\mathrm{pp})\mathrm{n}_{\mathrm{sp}}$ channel (with a cut on the missing mass to exclude pion production) naturally eliminates the πN and $\pi\pi N$ decay channels of these resonances. Moreover, the coplanarity built into this experiment favors the acceptance of the $(e, e'pp)$ SRC channel over that of any resonant decay channels, which tend to populate the phase space over 4π, a fact verified by Monte Carlo simulations that we have carried out.

2.4 Effects of FSI

The question of FSI (Figure 1c), and the associated modification of physics observables, is an issue for consideration. For our chosen kinematics, we assert that FSI comprise a non-dominant and calculable component of the total cross section in the $^3\mathrm{He}(\mathrm{e},\mathrm{e}'\mathrm{pp})\mathrm{n}$ channel.

The assertion of diminished FSI is strongly supported by the expectation that these processes are much smaller in ^{3}He than in large nuclei. On the theoretical front, recent calculations on the $A = 3$ system have made a significant step forward in the treatment of FSI [12, 17]. Specifically, the full calculations of *ppn* breakup from ^{3}He using realistic NN forces with full inclusion of all rescattering processes, and including all relevant NN force components, have been carried out. This procedure, which employs the solution of Faddeev-like integral equations, can be used to check the role of FSI via theoretical calculations. Depending on the kinematical conditions, a significant deviation from PWIA may be observed, but at least now a reliable theoretical treatment of FSI is possible at energy transfers typical of what we propose. The general trend is that FSI are diminished in importance as the momentum transfer increases. In addition, our chosen kinematics involve fairly small angles of the initial state protons; 27-35° in the centre of mass with respect to $\vec{q}$. This suppresses $NN \to N'N'$ quasi-free scattering, which constitutes the bulk of FSI. Additional suppression factors arise from restrictions on the missing momentum, missing energy, and the coplanarity between the three-momenta of the two ejected protons with respect to the momentum transfer vector, i.e. on the quantity $\vec{q} \cdot (\vec{p}_{p_1} \times \vec{p}_{p_2})$.

Finally, theoretical NN and π-N calculations are quite advanced. Indeed, accurate NN forces exist up to nucleon kinetic energies exceeding 1 GeV, and the Glauber method is used reliably to calculate FSI even above 1 GeV [18]. All these considerations justify the large values of q and the choice of kinematics selected for this work.

3 Existing Evidence for SRC

The first topical results from the medium-energy CW accelerators at NIKHEF, Mainz, and Bates on a variety of nuclei, have provided significant data on correlations in nuclei. As examples, we mention the experiments which studied the exclusive $^2H(e,e'p)$ at large missing momenta [19], as well as the semi-exclusive $^{12}\mathrm{C(e,e'p)}$ reaction [20]. The difficulties experienced in separating the various competing reaction mechanisms are discussed by the authors of these papers, and they concluded that the most effective technique for enhancing the contribution of SRC is to study the two-proton emission channel, $(e,e'pp)$. Indeed, this has been the path that has been followed recently, as described in references [21, 22, 23, 24].

3.1 Measurements of $(e,e'pp)$ at NIKHEF

We begin the review of the recent NIKHEF $^3\mathrm{He(e,e'pp)n}$ experiments by examining the missing momentum of the residual (A-2)-system, p_m. This is an important parameter in tuning the kinematics towards promoting the SRC component. In Figure 4, we show the differential cross-section for the $^3\mathrm{He(e,e'pp)n}$ reaction at $\omega = 220$ MeV and $q = 305$ MeV/c as a function of the missing momentum of the neutron [24, 25]. Also shown in the figure are continuum Faddeev calculations. The solid curve, which does **not** include any two-body hadronic currents, tends towards the data at low p_m, but significantly underestimates the data at high missing momentum. The dashed curve includes meson exchange currents, and shows that these form a small part of the cross section at low neutron missing momentum. The general behaviour shown here is not surprising, since large p_m signifies an "active" (non-spectator) third nucleon, which is consistent with processes such as 2BC, FSI, and three-nucleon absorption. We conclude here that **SRC can be reliable extracted only under the condition that p_m is consistent with Fermi momentum of the third nucleon** on ^{3}He, as already discussed in Section 2.3.

In Figure 5, we show differential cross-section results for the $^{16}\mathrm{O(e,e'pp)}$ reaction for three values of ω, and a single value of $q = 305$ MeV/c [24, 26]. The upper panels correspond to the ground state of the residual nucleus, while the lower panels to the lowest 2^+ excited state of ^{14}C. There are a number of important features to point out. First, we note that the agreement with the full theoretical calculations of the Pavia group, which includes SRC as well as traditional 2BC processes, is striking for the ground state scattering. This fact gives further credence to the claim that focusing on an exclusive channel, where the quantum numbers of the residual system are explicitely known, is most effective. Second, the contribution of the 2BC processes increases with increasing ω. Finally, we note that the signature for SRC here is the specific $L = 0$ dependence in the cross-section, suggesting the dominant role for the knockout of a pair of nucleons in a relative S-state, driven by SRC.

While these results from NIKHEF are impressive, the authors note an issue of concern; in the $\omega = 240$ MeV region the Δ is increasingly important as evidenced by the fact that the contributions from two-body currents (dotted lines in the upper three panels of Figure 5) approach those from one-body currents (dashed lines). Thus, in this proposal we have chosen to measure on the low ω side of the quasi-elastic peak, away from the Δ-resonance. This is feasible only with the high energy, high duty

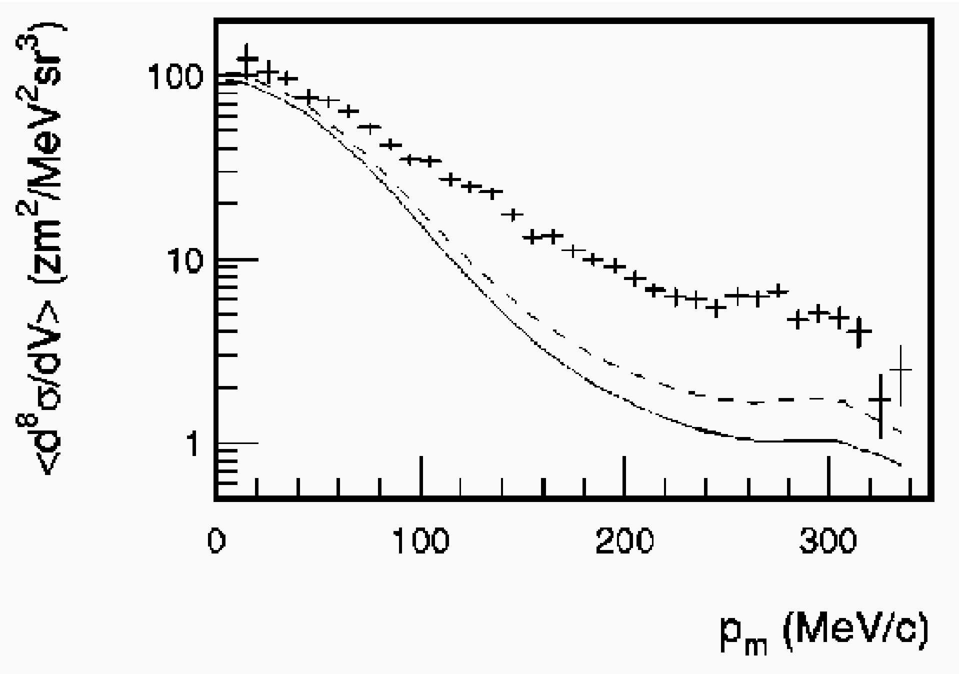

Figure 4: Cross-Section for the ^{3}He(e, e′pp)n reaction from NIKHEF. The curve represents the results of a continuum Faddeev calculation, from reference [17].

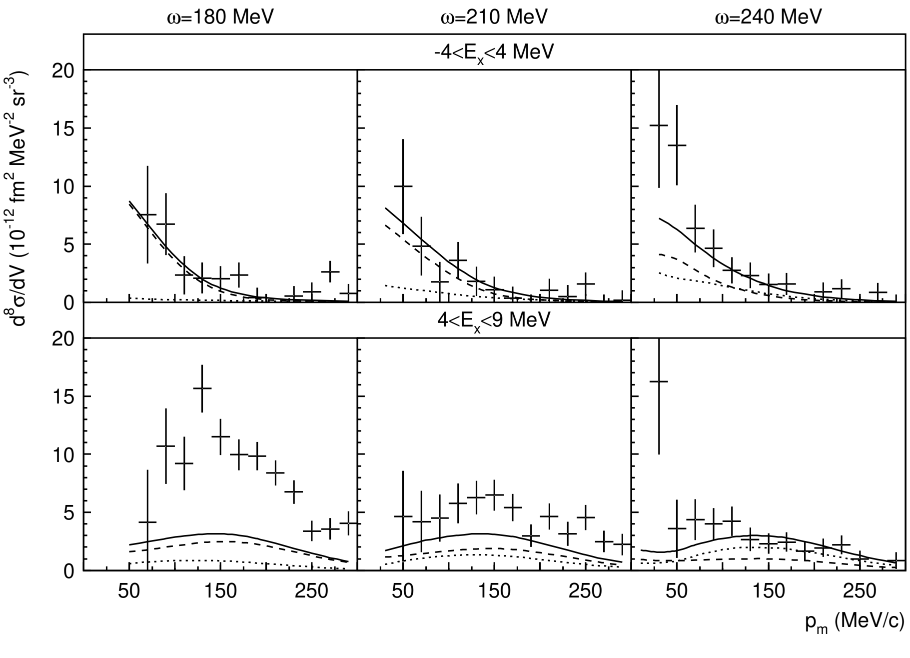

Figure 5: Cross-Section for the ^{16}O(e, e′pp) reaction from NIKHEF. The solid curves represent calculations of the Pavia group [27], with the dashed (dotted) curves indicating the contribution of the one- (two-) body hadronic current.

factor electron beam and high momentum spectrometers available in Hall A.

Based on this evidence, we ascertain the **requirements of the SRC pursuit**:

- a kinematically complete experiment in the $(e, e'pp)$ channel
- optimized kinematics where 2BC processes do not contribute
- large relative momentum between the two outgoing protons
- small missing momentum of the residual system
- discrete detectors operating at a high luminosity

3.2 Correlation Studies in Hall B/CLAS

3.2.1 $^3He(e, e'pp)n$

Weinstein *et al.* [32] have recently measured the $^3He(e, e'pp)n$ reaction in CLAS with 2.2 and 4.4 GeV electrons, and have specifically selected events where one nucleon has most of the kinetic energy and has less than 300 MeV/c of momentum perpendicular to $\vec{q}$. Thus, it is inferred that this nucleon absorbed most of the transferred momentum and energy. When this is done, they see isotropic, back-to-back NN pairs with small average momentum along $\vec{q}$. They also measure the total and relative momentum distributions of these pairs and find that they do not depend significantly on isospin (*pp* vs. *pn* pairs) or on momentum transfer.

Interestingly, PWIA calculations reproduce many features of the data. Calculations by Glöckle [12] and by Ciofi degli Atti [13] indicate that the cross section depends primarily on the overlap integral between the continuum state and bound state of the NN pair. Neither meson exchange currents nor the final state rescattering of the leading nucleon appear to contribute to the cross section.

Thus, Weinstein *et al.* claim to have measured NN correlations in $^3He(e, e'pp)n$ without any significant contamination from other processes by striking the third nucleon and detecting the spectator correlated pair.

In Fig. 6, we show data from the CLAS analysis where cuts have been applied to select events where all three nucleons had momenta greater than 250 MeV/c, and one of the initial state nucleons had its momentum predominantly parallel to $\vec{q}$. In this case, the opening angle between the other two (spectator) nucleons is of interest. This angle is plotted for a) *pp* pairs with a leading neutron and b) *pn* pairs with a leading proton. A large peak at 180° (i.e., $cos(\theta) = -1$) in both figures. This back-to-back peak is a strong indication of correlated NN pairs.

Finally, in Fig. 7, we show data from the CLAS analysis after all cuts have been applied to select correlated initial state *pp* pairs. We note that the "relative momentum" which they use corresponds to the momentum of *each* proton in the initial state nucleus, and thus is equivalent to the internal momentum that we refer to later in this proposal. While it indeed appears that they have been able to

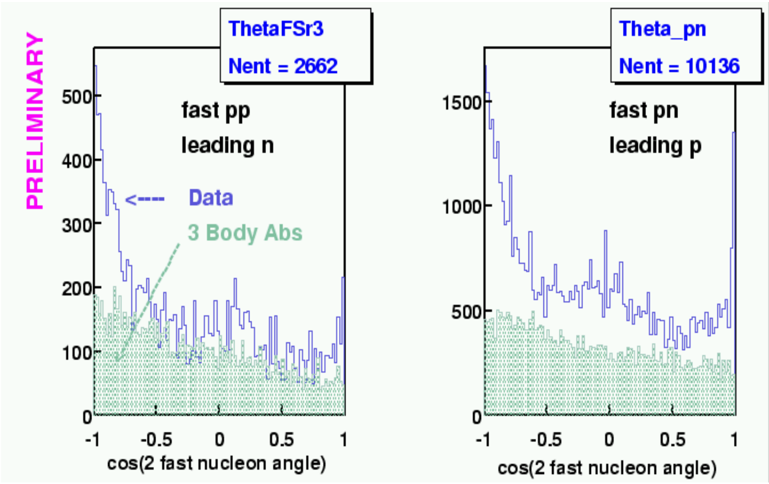

Figure 6: Opening angle between spectator nucleons in $^3He(e,e'pp)n$ measured in CLAS. The figure is from Ref. [32]

isolate correlated pairs, the statistics are too limited to further bin the data in recoil momentum for a more detailed analysis.

While the Hall B results are encouraging, we note that they have not yet extracted cross sections from the data, a task which is potentially fraught with difficulties relating to understanding the CLAS acceptance. A direct comparison of cross sections with theoretical calculations is crucial to the interpretation of underlying mechanisms which contribute. From our point of view, the most important conclusion of the Hall B analysis perhaps is that there exist optimum phase space regions for the study of SRC, where competing channels are greatly suppressed. Thus, a well designed experiment with discrete detectors, taking advantage of the higher luminosity possible in Hall A, can take advantage of this fact.

3.2.2 $A(e,e')$

Egiyan *et al.* [33] have invesigated cross sections for inclusive scattering from various nuclei with CLAS. Of particular interest is the extraction of the ratio,

$$R^A_{^3He} = \frac{3\sigma^A(x,Q^2)}{A\sigma^{^3He}(x,Q^2)}, \tag{1}$$

which according to calculations of Frankfurt *et al.* [34], should scale in the $1.3-1.4 < x < 2$ region, if $Q^2 > 1.5(GeV/c)^2$. The main point of this statement is a similarity of ^3He and heavier nuclei momentum distributions in the $p_i > 0.4GeV/c$ region, because the events with $p_i > 0.4GeV/c$ come only from the nucleon correlations.

In Fig. 8, we show the results of the CLAS analysis, where the above ratio is plotted comparing ^3He to both iron and carbon data. While the agreement with the theoretical predictions is fairly impressive, of particular interest is that the predicted

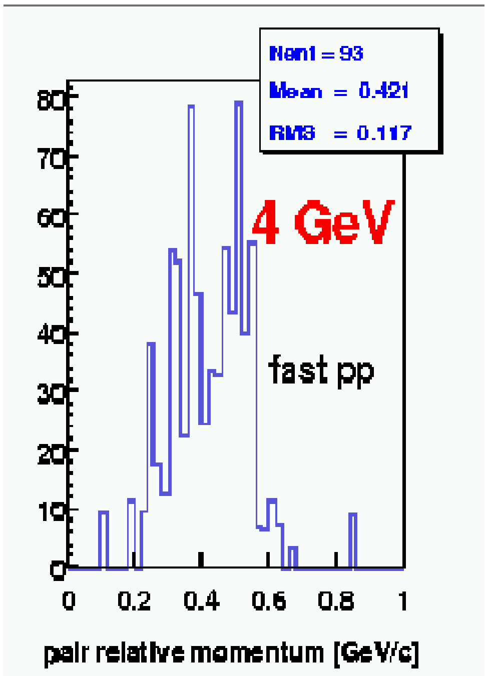

Figure 7: Relative momenta of correlated pp pairs from $^3He(e,e'pp)n$ in CLAS. The figure is from Ref. [32]

scaling occurs at an x-value approximately in the middle of the range of x covered in our proposal ($1.2 < x < 2.0$). As well, the Q^2 values that we have chosen are approximately the same as in the CLAS data. Based on this, we conclude that we will measure in kinematic conditions which will be favored by initial state correlations.

3.3 Comparison to E01-015 - $^{12}C(e,e'pN)$ Reactions in the $x > 1$ Region

Our proposal is closely related to the previously approved Hall A proposal E01-015 to study SRC in ^{12}C. In total, 550 hours of beam time was allocated to this experiment. An important question is: why should we do another measurement with similar goals? The most important issue is the interpretation of the final results.

Data from our experiment would provide significant help in interpretation of the E01-015 data. As an example, we point to the study of inclusive data from CLAS described earlier. Combining the results of E01-015 with the results of our experiment would be quite interesting in this sense. Also, due to the similarity in proposed kinematics, such a comparison is meaningful. As well, understanding a simpler system such as ^3He is beneficial in trying to understand a more complicated one, such as carbon.

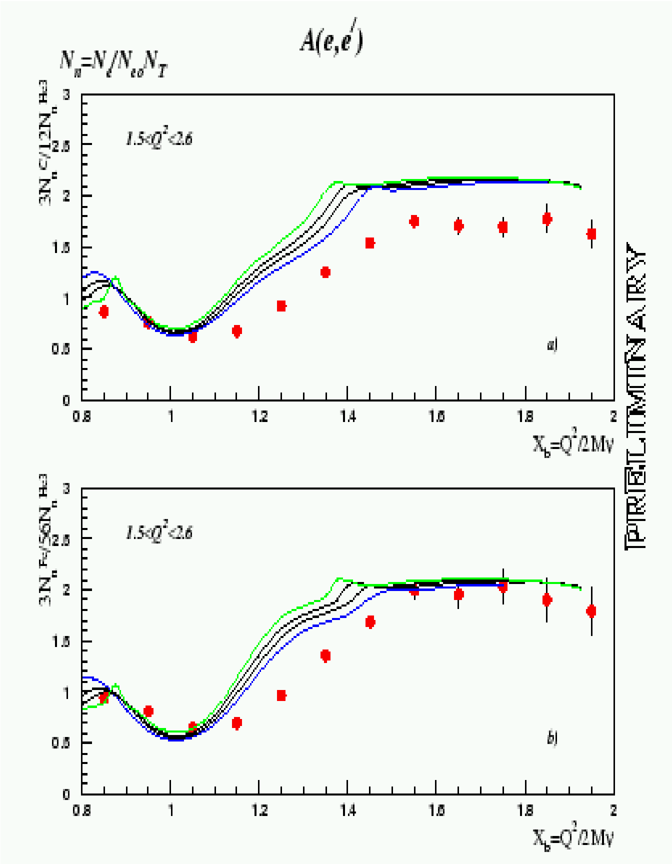

Figure 8: Data for $^3He(e,e')$, $^{12}C(e,e')$, and $^{56}Fe(e,e')$ from CLAS. The different theory curves span the range of Q^2 of the data (Green - $Q^2 = 1.5GeV^2$, Blue - $Q^2 = 2.6GeV^2$). The figure is from Ref. [33]

We note that our selected range of p_{miss} is shifted by approximately 50 MeV/c compared to E01-015. Both experiments are in a region where one can expect to see correlated NN pairs. We plan to achieve similar statistical accuracy to E01-015 over the range of p_{miss}, except in the lower p_{miss} region which we do not cover in this proposal. Due to much higher luminosity, we expect to be able to do this in about 40% of the time allocated to the E01-015 experiment.

3.4 Summary of Physics Justification

The central objective of this Proposal is the extraction of a direct signature for SRC. We believe that in the nucleonic picture, this signature exists only in the framework of a theoretical prediction. In the end, we must compare our data to the best theory we have to understand it. Thought of another way, our data will serve to provide constraints and input for modern theories which include SRC effects.

As an example, we point to a modern ^3He spectral function, such as the one calculated in [30], which is constructed using realistic NN potential. The NN potential used has a full description of the NN interaction (including a short range parametrization of the repulsive core). Thus, any enhancement that one sees in the data at high p_{miss} over what is predicted by the spectral function in a PWIA framework can be due to either:

1. Physical NN correlations which are not accounted for in the NN potential.

2. The breakdown of the PWIA framework itself. This is most likely in the form of FSI (not included in the PWIA/spectral-function framework). We note that this is the culprit that stalled the early excitement about finding unique signatures of SRC in $(e, e'p)$ data early on.

3. Contributions from traditional 2BC.

We are seeking a direct dynamical signature of the effect of the short-range repulsive core. The goal is to find the contribution of such short-range (high momentum) correlations directly in a reaction, such that we can construct a theoretical framework which is consistent with what is seen to be needed in nuclear matter calculations.

Therefore, the purpose of our proposal is to isolate SRC in a kinematical region where 2BC are small and FSI are under control by means of full calculations. Extracting *pure* signatures of SRC should enable us to understand better the reaction mechanism (quark exchange, heavy meson exchange, etc.) which is responsible for the repulsive core.

4 The Experiment

4.1 The Choice of Energy Transfer Region

There are a number of factors underlying the optimal choice of the ω region for this experiment, explained below.

At the quasi-elastic region, SRC investigations in the $(e, e'pp)$ channel are hindered by the fact that the energy and momentum transfers are small. This results in small relative momenta between the two ejected protons, a feature that diminishes the effect of SRC, since these are coupled to high relative momenta.

In the "dip" region (between the quasi-elastic peak and the Δ resonance), there is no doubt that the the experimental data clearly indicate more strength than the basic *e-p* interaction can account for. The magnitude of the missing strength in this region varies among different models, and some can account for this strength, provided that several mechanisms are taken into consideration [28]. Unfortunately, calculations indicate that the Δ resonance is one of the dominant contributors. It is for this reason that we have chosen to avoid this region, and concentrate instead on the lower ω side of the quasi-elastic peak.

Having said this, choosing a fairly low energy transfer, while at the same time having fairly high three-momentum transfer (necessary to probe large internal momenta), results in a number of experimental requirements:

- The three-momentum transfer, $\vec{q}$, must be absorbed by the initial state proton that was initially travelling largely anti-parallel to $\vec{q}$.
- At the same time, the struck initial state proton cannot be travelling exactly anti-parallel to $\vec{q}$, for this would result in a situation where the two final state protons would be emitted in the same direction in the lab, which would make detection of both protons extremely difficult. As well, it seems clear that if both final state protons are emitted in the same direction, and with comparable momentum, FSI would become increasingly large.
- Our final choice of kinematics reflects this compromise; the opening angle between the final state protons in the lab frame is approximately 47°, which is dictated in the end by the minimum physically acheivable opening angle between HRSH and BigBite.

It is also important to note that while SRC have both longitudinal and transverse parts, traditional 2BC are transverse by nature, and thus choosing high ϵ, which of course will result from low ω, high $\vec{q}$, and large Q^2, results in suppressing the 2BC contribution.

4.2 The Target Nucleus (^{3}He)

The nature of SRC dictates a target of high nuclear matter density, but low A. The latter requirement stems from pion absorption results from TRIUMF and LAMPF, which indicated that nuclei heavier than ^6Li complicate the picture significantly due to increased FSI complications.

In addition, since the SRC cross sections are expected to be small, any uncertainties in the angular correlations and missing four momentum information will complicate the analysis, perhaps even to the point of loss of information. We thus require a **kinematically complete experiment**, at least in the first step on the road to understanding SRC. This will allow us to restrict our measurements to regions of phase space where the momentum distribution of the neutron is consistent with a spectator (Fermi) momentum, in order to ensure that the energy and momentum transfer in the reaction were entirely absorbed by the two-proton cluster. Clearly, one has to resort to a triple-arm experiment on ^{3}He to achieve all this. In fact, the ^{3}He(e, e′pp)n reaction is not only kinematically complete, it is over-constrained.

Theoretically, ^{3}He is a very attractive target: it has well described ground state and continuum wavefunctions, and the electrodisintegration of ^{3}He can be treated fully by solving Faddeev-like integral equations, using realistic NN forces [17]. The inter-nucleon distance in ^{3}He is not that much different than heavier nuclei and thus the SRC signatures should be strong enough to manifest themselves. The choice of ^{3}He as a target has received the strong endorsement of J.M. Laget, J.A. Tjon, W. Glöckle, and R. Schiavilla, in our communications with them.

We mention here that although valuable insights have been obtained from the ^{12}C(e, e′pp) and ^{16}O(e, e′pp) experiments at NIKHEF and Mainz, their deconvolution relies heavily on theoretical calculations. Several of these are becoming state-of-the-art efforts. However, we assert that the interpretation our $^3\mathrm{He}(\mathrm{e},\mathrm{e}'\mathrm{pp})\mathrm{n}_{\mathrm{sp}}$ proposed experimental results will be the least model-dependent, due to outright suppression of competing reaction mechanisms. **The $^3\mathbf{He}(\mathbf{e},\mathbf{e}'\mathbf{pp})\mathbf{n}_{\mathbf{sp}}$ channel proposed here will provide the cleanest SRC signature among all similar efforts.**

For this experiment, we plan to use a ^3He target provided by the California State, Los Angeles (CSULA) group. This group has already successfully designed and installed the so-called "tuna can" ^3He target in Hall A. While this target is now a standard facility in Hall A, it turns out that for detection of the more backward proton with BigBite, we require a target which will allow vertical exit angles of $\pm 300\ mr$. The CSULA group, together with the JLab design team, has recently designed such a target, with a so-called "racetrack" footprint, that will be used for other already approved experiments in Hall A. Of course, this target will make use of much of the currently available cyrotarget infrastructure.

4.3 The Detectors

The electron and forward going proton will be detected in the $HRSE$ and $HRSH$ Hall A spectrometers, respectively. These devices will be operated in their standard configuration. We propose to use the Big Bite spectrometer as the third arm in this experiment [31]. This device subtends a 100 msr solid angle and accepts momenta between 300-900 MeV/c, values that are compatible with this experiment, with the added advantage of lower susceptibility to background.

4.4 Kinematics

The proposed optimal kinematics for this experiment are shown in Tab. 1, as deduced and calculated from the above arguments. We have run Monte Carlo simulations using MCEEP to calculate double $(e, e'p)$ coincidence rates. In all results that we report, we have used the Salme spectral function for ^3He [30]. These simulations produce kinematic distributions of the recoiling (A-1) system. We have assumed the spectator neutron approximation, and that at these internal momenta all triple coincidences will be due to correlated pp pairs in the initial state wavefunction.

In Tab. 2, we show the various experimental parameters which have been used in the simulations, along with the expected number of events for $(e, e'p)$, in the two- and three-body breakup channels, as well as the $(e, e'pp)$ triple coincidence counts. We note that in these kinematics, the $(e, e'p)$, in both two-body and three-body

E_e MeV	E_e' MeV	Q^2 GeV^2	θ_e deg	p_p MeV/c	θ_p deg	θ_{BB} deg	p_{miss} MeV/c	ϵ	θ_q deg
4500	3892.8	1.742	18.1	1068	43.3	90.0	480	0.942	59.8
4500	3918.2	1.75	18.1	961	41.2	88.5	588	0.943	57.5

Table 1: Kinematics 1 and 2

Target density	0.08 g/cm^3
Target length total	10 cm
Target length used	7 cm
Beam current	100 μA
Momentum acceptance in HRS	$\pm$ 4.5%
Collimators in HRS	6 msr
BigBite ang. acceptance	96 msr
BigB. mom. accept. used for kinem 1(2)	350-550 (450-700) MeV/c
Beam time requested for kinem. 1(2)	70 (160) hours
Number of expected events:	
Number of $^3He(e,e'p)pn$ events for kin. 1(2)	14200 (10000) events
Number of $^3He(e,e'p)d$ events for kin. 1(2)	1200 (700) events
Number of $^3He(e,e'pp)n$ events for kin. 1(2)	6700 (6200) events

Table 2: Experimental Parameters and Rates for Kinematics 1 and 2

breakup channels, has never been measured before and is very interesting in and of itself. Thus, this is an additional quantity which can be extracted in this experiment.

In Fig. 9, we show results of MCEEP simulations of the $^3He(e,e'p)$ reaction in the above kinematics. To be clear, the missing energy and missing momentum shown refer to the recoiling (A-1) system. In the spectator neutron approximation the missing momentum corresponds to the internal momenta of each proton in the initial state correlated *pp* pair. We can confirm immediately that the spectral function used does not include pion production channels, as evidenced by the fact that almost all events lie below the 140 MeV missing energy threshold. Events which lie above this threshold must be due to energy loss in the target or elsewhere. The main point is that very few interesting events will be lost by placing a cut on missing energy below the pion production threshold. All triples rates that we have calculated correspond to missing energies below this threshold (see Fig. 9).

In Fig. 10, we show the kinematic coverage in the experiment. It is clear that at higher values of x we probe larger values of internal momenta. We note also that the range of x coverage is similar to E01-015, which will measure in similar kinematics on a carbon target. Thus, a direct comparison between the results of this experiment and the carbon experiment will be possible. Figure 10 presents results for the range of angles between the q vector and the axis of the initial state *pp* pair. Finally, in Fig. 11, we show the effect of the BigBite acceptance on the triple coincidence rate. We note that in the chosen kinematics, the angular acceptance of BigBite matches

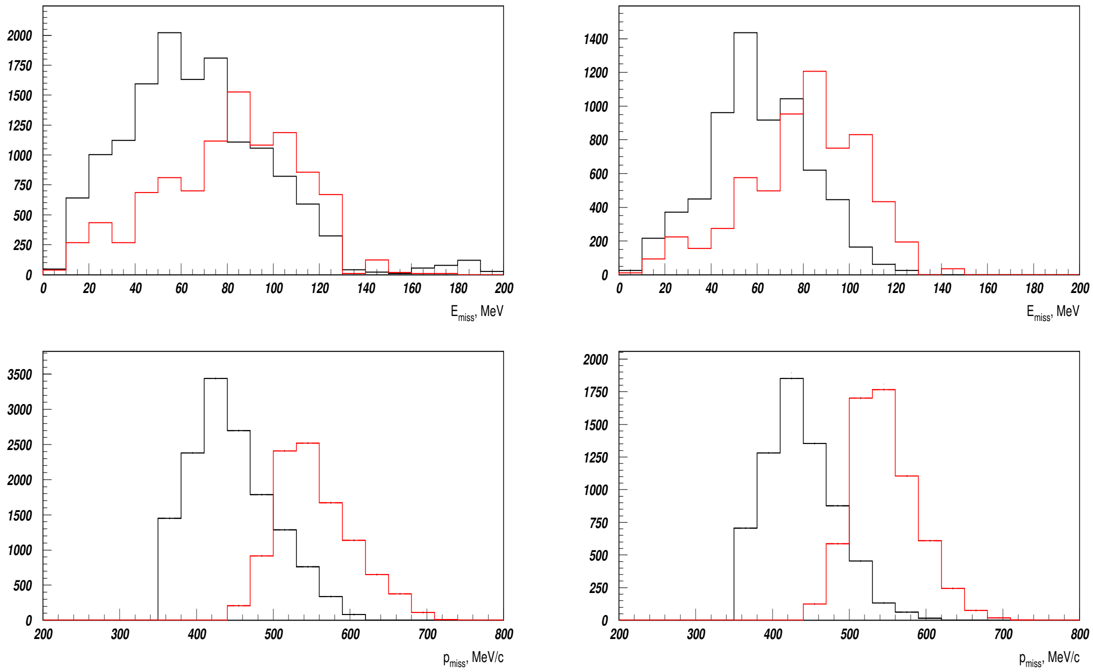

Figure 9: MCEEP simulations of the $^3He(e,e'p)$ reaction. Left panels: The missing energy and momentum shown refer to the recoiling (A-1) system. Right panels: Cuts to select second protons detected in BigBite were applied: The missing energy and momentum shown refer to the recoiling (A-1) system. Kinematics 1 is shown in black, and Kinematics 2 is shown in red.

well with the range of angles predicted for the second proton.

4.5 Accidental Rates and Signal to Noise Ratio

Table 3 shows singles rates for (e,e'), (e,π^-), (e,p), and (e,π^+) calculated from the EPC and QFS codes of Lightbody and O'Connell. In Tab. 4, we show the associated random coincidence rates, assuming a 100 ns coincidence window. In addition, we calculate the real/accidental signal to noise ratio assuming a coincidence timing peak of 2 ns width. We see that the accidental coincidence rates in the coincidence timing peak are small compared to the real rates.

We plan to make use of the new trigger scintillator array for BigBite which is being provided by the Glasgow group. We plan to turn off the scintillator paddles in the trigger plane associated with momenta outside of the useful range for the second proton. The singles proton rates in BigBite are quite large on the low momentum side of the focal plane, and since we are not interested in particles in this momentum

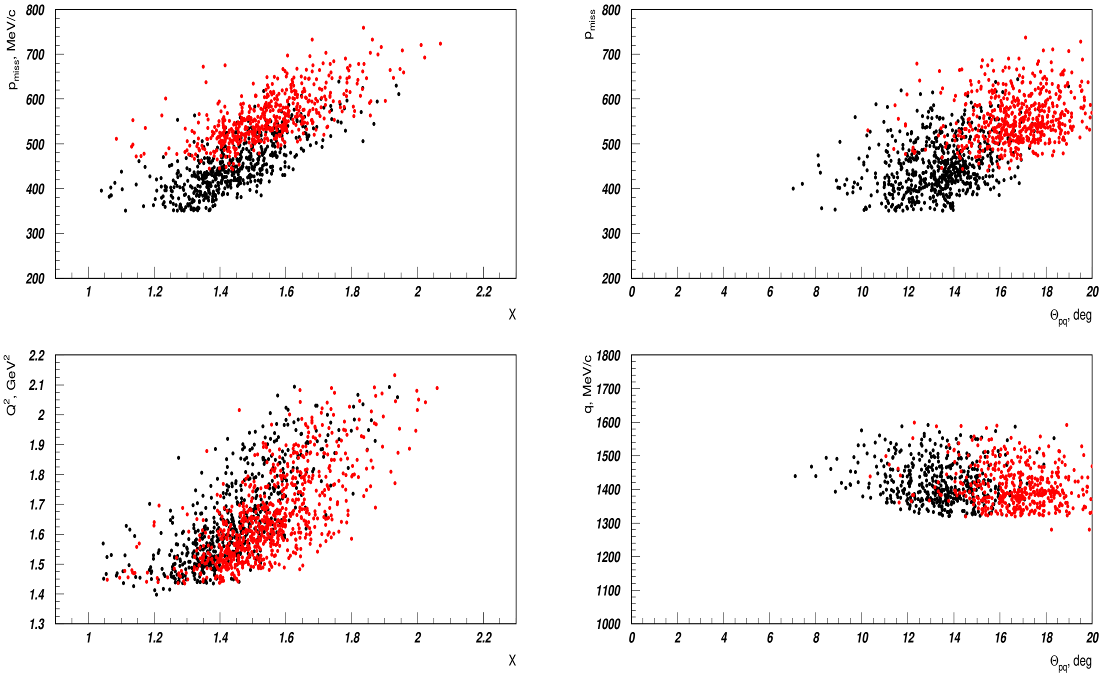

Figure 10: Left panels: Kinematic coverage from MCEEP simulations. Right panels: Range of θ_{pq} from MCEEP simulations. Kinematics 1 is shown in black, and Kinematics 2 is shown in red.

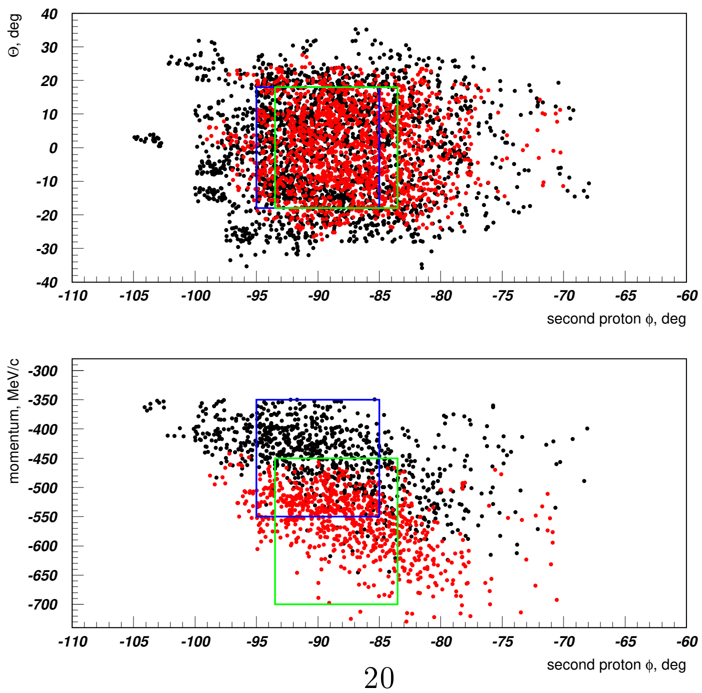

Figure 11: Effect of BigBite Acceptance. Kinematics 1 is shown in black, and Kinematics 2 is shown in red.

E-arm	H-arm	H-arm	BigBite	BigBite
(e,e′) Hz	(e,π^+) Hz	(e,p) Hz	(e,π^+) Hz	(e,p) Hz
75	3.4×10^4	1.3×10^5	2×10^6	7.6×10^6
42	3.4×10^4	1.5×10^5	2×10^6	7×10^6

Table 3: Single background rates: EPC code of J.S. O'Connell and J.W. Lightbody used to estimate the (e,$\pi-$), (e,$\pi+$), and (e,p) rates. (e,$\pi-$) rates were found to be negligible. (e,e′) were rates based on the QFS code estimate.

Real	Random	Signal/noise	Real	Random	Signal/noise
(e,e′p) Hz	(e,e′p) Hz	(e,e′p)	(e,e′pp) Hz	(e,e′pp) Hz	(e,e′pp)
0.079	1	3.9	0.037	0.003	12
0.024	0.62	2	0.015	0.00085	18

Table 4: Coincidence rates: random (e,e′p) rates are given for coincidence window Δt = 100 ns, but signal/noise ratio was calculated assuming a 2 ns (5 ns) peak for double (triple) coincidences; a correction was made to account for real events outside the ±3.5 cm cut on target length.

range, it will be helpful to disable these paddles. Second, as in E01-015, which will measure *pp* and *pn* triple coincidence cross sections on carbon (using BigBite and a neutron array for the second nucleon), we will not use the MWPC chambers of BigBite. Our momentum and angular resolution requirements for the second proton are modest, and thus wire chamber information is not needed. Thus, issues of high rates in the wire chambers are eliminated from consideration.

4.6 Beam Time Request

We present a summary of the beam time requested in Tab. 5. We wish to obtain 3-5% statistics in each of approximately 10 bins over the momentum range of the second proton (to be detected in BigBite). Our previous experience in extracting cross sections for $(e,e'p)$ on light nuclei in Hall A tells us that obtaining 5% systematic uncertainties is quite reasonable, and thus we have matched the statistical uncertainties to the expected systematics. We have also requested approximately one shift for optics calibrations of the HRSE and HRSH spectrometers at the specific momenta of this experiment. Again, experience dictates that this will prove very useful in extracting cross sections in Hall A.

Kinematical Setting	Number of Beam Hours
Calibration	10
Kinematics 1	70
Kinematics 2	160
Total:	240

Table 5: Beam time request (including optics and calibration studies)

5 Summary

In a direct manner, SRC probe quark degrees of freedom in the nuclear wavefunction. As well, in the nucleonic picture, SRC manifest themselves in the details of realistic NN potentials empoloyed in modern calculations of electron scattering from nuclei. As far as the physics goals addressed in this proposal are concerned, we will focus on a measurement in a specific region of phase space, in order to determine the nature of SRC and their contribution to the ground state nuclear wavefunction, and in specific kinematics which allow the measurement of large values of the relative momentum. These correlations can be only accessed directly via measurements at $x > 1$ in $^{3}\mathrm{He(e, e'pp)n_{sp}}$ channel. In these kinematics – where all other competing channels are suppressed – we will isolate the one-body current reaction mechanism, and will provide constraints to modern theoretical calculations which include full final state interactions.

References

[1] 10^{th} NIKHEF Mini-Conference on "Studies of Few-Body Systems with High Duty-Factor Electron Beams", NIKHEF, January 6-7, 1999.

[2] Fifth Workshop on "Electromagnetically Induced Two-Hadron Emission" Lund, Sweden, June 13 - 16, 2001.

[3] S. Auffret *et al.*, Phys. Rev. Lett. **55** (1985) 1362.

[4] T. Emura *et al.*, Phys. Rev. **C49** (1994) R597.

[5] T. Emura *et al.*, Phys. Rev. Lett. **73** (1994) 404.

[6] C. Marchand *et al.*, Phys. Rev. Lett. **60** (1988) 1703, J.J. van Leeuwe, *et al.*, Nucl. Phys. **A 631** (1998) 593c, J.M. Le Goff, *et al.* Phys. Rev. C **50** (1994) 2278.

[7] Th.S. Bauer, Nucl. Phys. **A546** (1992) 181c.

[8] Hall A Few-Body Working Group Meeting, Jefferson Lab, May 23, 1999.

[9] J.M. Laget, Phys. Rev. **C35** (1987) 832.

[10] L.L. Frankfurt *et al.*, Phys. Rev. **C56** (1997) 1124.

[11] J. Ryckebusch, Laboratory for Nuclear Physics, University of Gent, Internal Report SSF95-12-01.
J. Ryckebusch, "Workshop on Electron Nucleus Scattering", Elba International Physics Center, July 1-5, 1996.

[12] W. Glöckle et al., Fifth Workshop on "Electromagnetically Induced Two-Hadron Emission" Lund, Sweden, June 13 - 16, 2001.

[13] C. Ciofi degli Atti and L.P. Kaptari, Fifth Workshop on "Electromagnetically Induced Two-Hadron Emission" Lund, Sweden, June 13 - 16, 2001.

[14] V.D. Efros *et al.*, Phys. Rev. **C58** (1998) 582.

[15] R.E.J.. Florizone *et al.*, Phys. Rev. Lett. **C58** (1999) 2308.

[16] E. van Meijgaard and J.A. Tjon, Phys. Rev. **45** (1992) 1463.

[17] J. Golak *et al.*, Phys. Rev. **C51** (1995) 1638.

[18] S. Jeschonnek and T.W. Donnelly, Phys. Rev. **C59** (1999) 2676.

[19] W.J. Kasdorp, Ph.D. Thesis, University of Utrecht (1997); Few-Body Systems, in press.

[20] J.J. van Leeuwe, Ph.D. Thesis, University of Utrecht (1996); submitted to Phys. Rev. Lett.

[21] L.J.H.M. Kester *et al.*, Phys. Rev. Lett. **74** (1995) 1712, L.J.H.M. Kester, Ph.D. Thesis, Free University of Amsterdam, 1993, unpublished.

[22] G.J.G. Onderwater *et al.*, Phys. Rev. Lett. **78** (1997) 4893.

[23] G.J.G. Onderwater *et al.*, Phys. Rev. Lett. **81** (1998) 2213.

[24] D. L. Groep *et al.*, Phys. Rev. Lett. **83** (1999) 5443.

[25] D. L. Groep *et al.*, Phys. Rev. **C63** (2000) 014005-1.

[26] R. Starink, Ph.D. Thesis, Free University of Amsterdam, 1999, unpublished.

[27] C. Giusti *et al.*, Phys. Rev. **C57** (1998) 1691.

[28] M.J. Dekker *et al.*, Phys. Lett. **289B** (1992) 255.

[29] J.M. Laget, private communication.

[30] A. Kievsky, E. Pace, G. Salme, and M. Viviani, Phys. Rev. C 56, (1997), 64.

[31] D.J.J. de Lange *et al.*, Nucl. Instr. Meth. in Phys. Res. **A406** (1998) 182; *ibid.*, **A412** (1998) 254.
K. de Jager, private communication.

[32] L. Weinstein for the CLAS Collaboration, Fifth Workshop on "Electromagnetically Induced Two-Hadron Emission" Lund, Sweden, June 13 - 16, 2001.

[33] K. Egiyan for the CLAS Collaboration, Fifth Workshop on "Electromagnetically Induced Two-Hadron Emission" Lund, Sweden, June 13 - 16, 2001.

[34] L.L. Frankfurt, M.I. Strikman, D.B. Day, M.M. Sargsian, Phys. Rev. C56 (1993) 2451.